NIST copyright disclaimer

Multi-pulse fitting of Transition Edge Sensor signals from a near-infrared continuous-wave source

Jianwei Lee,[1] Lijiong Shen,[1,2] Alessandro Cerè,[1] Thomas Gerrits,[3] Adriana E. Lita,[3] Sae Woo Nam,[3] and Christian Kurtsiefer[1,2,a]

[1] Center for Quantum Technologies, National University of Singapore, 3 Science Drive 2, Singapore, 117543

[2] Department of Physics, National University of Singapore, 2 Science Drive 3, Singapore, 117542

[3] National Institute of Standards and Technology (NIST), 325 Broadway, Boulder, Colorado 80305, USA

(Dated: 10 June 2018)

Transition-edge sensors (TES) are photon-number resolving calorimetric spectrometers with near unit efficiency. Their recovery time on the order of microseconds limits the number resolving ability and timing accuracy in high photon-flux conditions. This is usually addressed by pulsing the light source or discarding overlapping signals, thereby limiting its applicability. We present an approach to assign detection times to overlapping detection events in the regime of low signal-to-noise ratio, as in the case of TES detection of near-infrared radiation. We use a two-level discriminator, inherently robust against noise, to coarsely locate pulses in time, and timestamp individual photoevents by fitting to a heuristic model. As an example, we measure the second-order time correlation of a coherent source in a single spatial mode using a single TES detector.

I. INTRODUCTION

detection in the optical band

Transition-edge sensors are wideband photon-number resolving light detectors that can be optimized for high quantum efficiency (> 98%) and to work in different regions of the electromagnetic spectrum, from soft X-rays to telecom wavelengths[1,2]. Their high single photon quantum efficiency was instrumental in one of the recent loophole-free experimental violation of Bell's inequality[3]. Absorption of a single photon by the TES generates an electric pulse response with a fast (tens of nanoseconds) rising edge, and a relaxation with a time constant of a few microseconds[4]. Photodetection events with time separation shorter than the pulse duration overlap and cannot be efficiently identified by threshold crossing. To avoid this problem, TES are often used with pulsed light sources with repetition rate lower than few tens of kHz[5]. This may exclude the use of TES with its superb detection efficiencies from some applications. In this work we therefore investigate the time discrimination for overlapping signal pulses for continuous-wave (CW) light sources. Similar problems are common in high-energy physics, and it was fundamental to study some of the several methods already developed [6–10]. Fowler et al.[10] improved time discrimination by considering the time derivative of the signal to locate the steep rising edge of individual photodetection events. In cases with high signal-to-noise ratio, as in the detection of high-energy photons like γ and X-rays (SNR $\approx$ 260, estimated from[10]), this approach is effective also when signals overlap. For near-infrared (NIR) photodetection with TES, it is necessary to filter high frequency noise components to *However,*

improve the signal-to-noise ratio (SNR $\approx$ 2.4, estimated from[4]) at the expense of a reduced timing accuracy. We approach the problem by separating it into two distinct phases: an initial coarse event identification, followed by a more accurate time discrimination. We identify photodetection events using a two-level discriminator. Its resilience to noise allows us to coarsely locate both isolated and overlapping pulses with a moderate use of filtering, thus retaining some of the high frequency components of the signal, useful to improve the time accuracy of the subsequent operations. For every detection region we estimate the number of photon-events from the total pulse area. This is possible only for monochromatic sources, with every detection event having the same energy. From the number of photons, we calculate a heuristic model function and fit it to the signal to recover the detection-times.

timing?

photons?

II. ELECTRONICS AND PHOTON DETECTION PULSE

no trade names, companies, etc unless recally necessary

Our

The Tungsten-based TES[11] ~~we use for this work~~ is kept at a temperature of 75 mK using an adiabatic demagnetization refrigerator cryostat ~~(Entropy Cryogenics)~~, and is voltage biased within its superconducting-to-normal transition in a negative electro-thermal feedback[12]. The detection signal is inductively picked up and amplified by a SQUID Series Array ~~(Magnicon C6)~~, followed by further signal conditioning at room temperature ~~(Magnicon electronics XXF-1[13])~~ with an overall amplification bandwidth of $\approx$ 6 MHz. We operate the the SQUID in a flux-locked loop to minimise low frequency components of the noise[13]. To characterize the TES response, we use a laser diode centered at 810 nm as a light source, operated in CW mode. We control the average photon

[a] christian.kurtsiefer@nus.edu.sg

 # you should mention about the overlapping events that cannot be discriminated by the TES and look like 2-photons. This work here addresses this problem
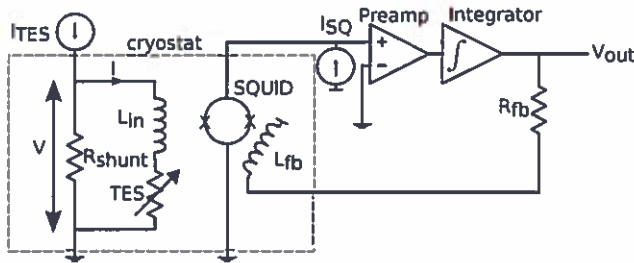
FIG. 1. Schematic of the TES readout circuit. The TES is voltage-biased by a constant current source I_{TES} through shunt resistor $R_{shunt} \ll R_{TES}$. The SQUID array amplifier picks up changes in TES resistance from L_{in}. The signal is further amplified outside of the cryostat. Signal feedback via R_{fb} and coil L_{fb} linearizes the SQUID response.
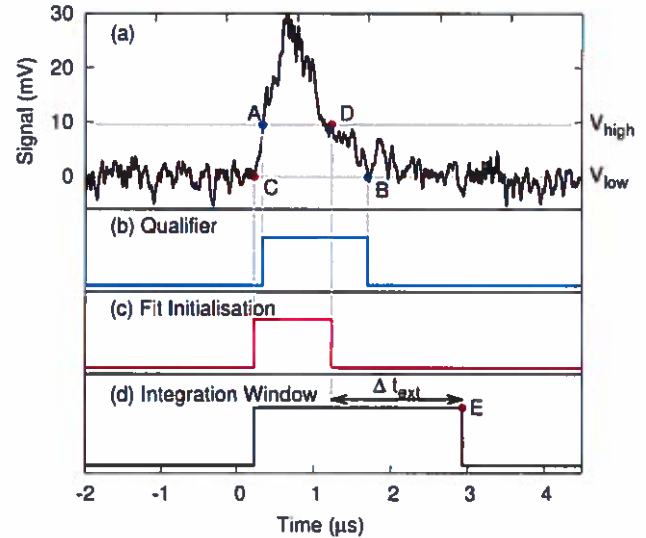

FIG. 2. (a) Typical TES signal trace with overlapping pulses. The horizontal lines show the high and low threshold settings of the Schmitt trigger mechanism. (b) Qualifying interval AB identified by the Schmitt trigger. (c) A narrower interval CD includes the the rising edges of the overlapping pulses, and is used to initialize a least-square fit. (d) A wider interval CE includes the rising edge and decaying tail, is used to estimate the number of photons associated with the event. Point E is obtained by extending interval CD by Δt_{ext}.

flux with a variable attenuator, then launch the light into a single mode fiber (type SM28e) that directs it to the sensitive surface of the TES.

We record $10\,\mu s$ long traces with a sampling rate of $0.5\,GS/s$ and a vertical resolution of $12\,bit$. For light at 810 nm, the signal generated by discrete absorption processes for each photon after the amplifier chain exhibits a rise time for a single photon pulse of $\approx 100\,ns$, and an overall pulse duration of $2\,\mu s$.

We collected a total of 4×10^5 traces with the TES continuously illuminated by an attenuated laser diode. Despite the flux-locked loop, we observe a residual vertical offset variation from trace to trace. For every recorded pulse trace $v'(t)$, we remove the residual baseline,

$$v(t) = v'(t) - V_M,\tag{1}$$

where V_M is the most frequently occurring value of the discretized signal $v'(t)$ over the sampling interval.

III. PULSE IDENTIFICATION

In a first step, we identify the presence of an absorption process from one or more photons in a trace, and distinguish it from background noise. This is done by a traditional Schmitt trigger mechanism[14], implemented via discriminators at two levels: a qualifier flag is raised when the signal passes threshold V_{high} (figure 2(a), point A) and lowered by the first subsequent crossing of threshold V_{low} (point B).

In order to minimize the number of false qualifier events, we consider a histogram of the maximum pulse heights for a sample of 4×10^4, traces shown in figure 3. The distribution has two distinct peaks, with one around 5 mV corresponding to traces without any detection event ($n = 0$), and another one starting from 9.5 mV onwards corresponding to traces with at least one detection event ($n > 0$). We choose V_{high} to the minimum between the two peaks (9.5 mV), and V_{low} to 0 mV.

An expected timing accuracy for single photon events that can be extracted from the TES signal would be given by the noise (about 1.75 mVrms), and the steepest slope of the response (0.11(9) mV/ns, estimated from an average of 10%-90% transitions of an ensemble of pulses) to be on the order of 16 ns. However, a simple threshold detection of the leading edge does not work if pulses start to overlap.

A more precise timing information of a photodetection event is obtained from a least square fit of the signal to a displaced standard pulse. To efficiently initialize this fit, we do not directly use the qualifier window AB for two reasons: first, it contains only a fraction of the leading edge belonging to the earlier pulse that contains most of the timing information, and second, it includes a large portion of the decaying tail unassociated with the onset of photodetection. The time window CD derived from the same discriminator levels ensures the inclusion of the first leading edge, and is shorter as well.

In a similar way, we derive an integration time window from the qualifier window to determine the pulse integral, from which we associate with the photon number of a quasi-monochromatic light source. As a starting point, we choose point C for the integration to capture the rising slope of a pulse, and extend the time D by a fixed amount Δt_{ext} to point E to capture the tail of the response signal (figure 2(d)). We found that it is more reliable to extend point D by a fixed time to capture the tail of the signal than to reference the end of the integration window to point B because the signal-to-noise ratio

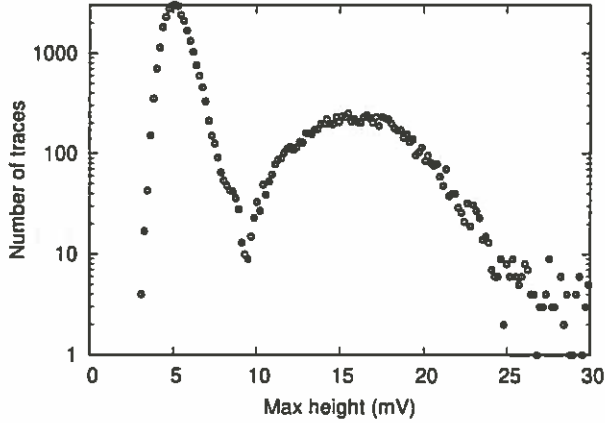*and to estimate our Schmidt trigger thresholds,*

FIG. 3. Distribution of signal maxima from a TES exposed to CW light from a laser diode. The two peaks correspond to no, and at least one detected photon, respectively.
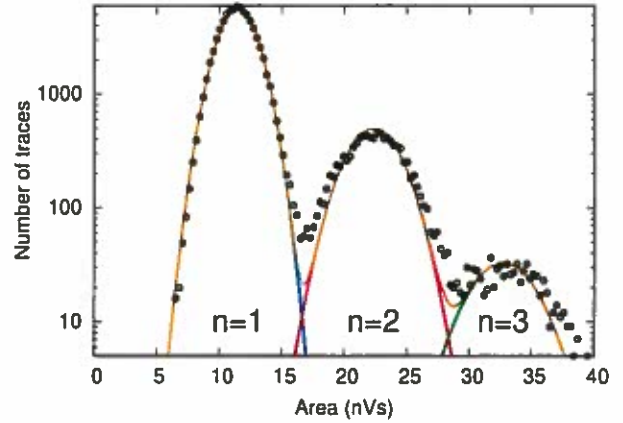

FIG. 4. Pulse area distribution of signals $H(a)$ identified within a single discriminated region. As described in detail in the main text, the continuous lines are Gaussian fits for the $n = 1$ (blue), $n = 2$ (red), and $n = 3$ (green) area distributions, and their sum (orange).

around B is low, leading to a large variation of integration times. We empirically find that $\Delta t_{ext} = 1700$ ns gives a good signal-to-noise ratio of the pulse integral. *Did you try any optimum filtering?*

IV. PHOTON NUMBER DISCRIMINATION

To determine the number of *photodetection events [photons?]* in an electrical pulse from the TES, we assume that the detection and subsequent amplification have a linear response, so that the integral of each signal is proportional to the energy absorbed[15], resulting in a discrete distribution of the areas of the signals. This distribution is spread out by noise, and we have to use an algorithm to extract the photon number in presence of this noise.

For this, we first compute the pulse area $a = \int_{t_C}^{t_E} |v(t)|$ for every qualified trace within region CE. Figure 4 shows a histogram of pulse areas from the qualified traces out of all the 4×10^5 acquired. The distribution shows three resolved peaks that suggest to be caused by $n = 1, 2, 3$ photons being absorbed by the TES.

One can fit the histogram in figure 4 to a sum of normalized Gaussian peaks $g_n(a; a_n, \sigma_n)$,

$$H(a) = \sum_{n=1}^{n_{max}=3} h_n \, g_n(a|a_n, \sigma_n), \tag{2}$$

where each Gaussian peak is characterized by an average area a_n and width σ_n. The ratio $a_2/a_1 = 1.95$ indicates that the TES response to photon energies of 1 and 2 photons is approximately linear.

We identify thresholds $a_{n-1,n}$ as the values that minimize the overlap between distributions $g_{n-1}(a|a_{n-1}, \sigma_{n-1})$ and $g_n(a|a_n, \sigma_n)$. With this, we assign a number of detected photons n by comparing the area of every trace to thresholds $a_{n-1,n}$ and $a_{n,n+1}$.

The continuous nature of the light source with a fixed power level makes it difficult to assign a number of photons per qualified signal, as the integration window *has a ~~series~~ [varies]* ~~variation~~ from pulse to pulse, and detection events may occur at random times in the respective integration windows. Heuristically, however, one could even replace the individual event numbers h_n in Eq. 2 by a Poisson distribution,

$$h_n = Np(n|\bar{n}), \tag{3}$$

where $\bar{n}$ is an average photon number, $p(n|\bar{n})$ the Poisson coefficient, and N is the total number of traces. For the data shown in figure 4, this would lead to an average photon number of $\bar{n} \approx 0.3$ per integration time interval.

V. DETERMINING THE DETECTION-TIMES OF OVERLAPPING PULSES

The difficulty of assigning a photon number to light detected from a CW source can be resolved if one treats the first detection process of light following the paradigm of wideband photodetectors in quantum optics[16]. As TES are sensitive over a relatively wide optical bandwidth, the corresponding time scale of the ~~the~~ absorption process that is much shorter than the response time scales of a few 100 ns of the TES device physics. Then, the signal would correspond to a superposition of responses to individual absorption processes, which may happen at times closer than the characteristic pulse time.

To recover absorption times of individual absorption events in a trace of N overlapping pulses, where N is determined with the pulse area method outlined in the previous section, we fit the TES response signal $v(t)$ to a heuristic model $v_N(t)$ of a linear combination of single-
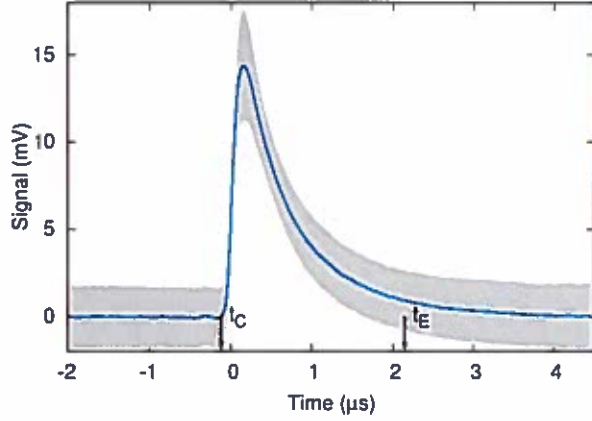
FIG. 5. Blue line: average response of TES and amplification to a short single photon pulse. We use a Schmitt trigger to identify the region between t_C and t_E. The pulse integral in this region is proportional to the average energy absorbed by the detector due to a single photon. Grey region: one standard deviation due to noise on the observed ensemble of N_1 traces.
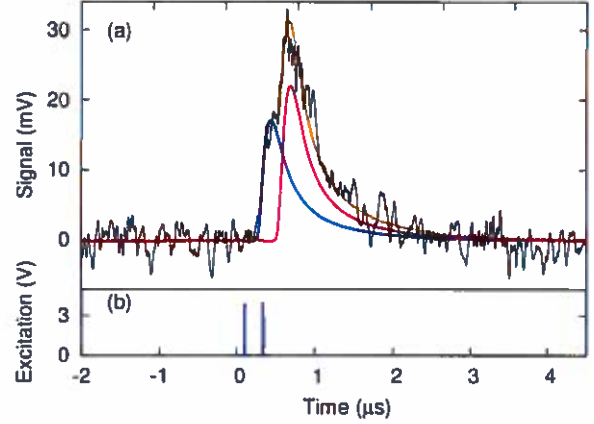

FIG. 6. (a) Fit of a two-photon signal with heuristic function described in the main text. Black line: measured TES signal after removing the vertical offset. Orange line: fit to Eq. (4), with two single photon components separated in time (blue and red line). (b) Electrical pulse pair separated by 239 ns sent to the LD illuminating the TES.

photon responses $v_1(t)$,

$$v_N(t|\{t_i, A_i\})) = \sum_{i=1}^{N} A_i \, v_1(t - t_i), \qquad (4)$$

where A_i is the amplitude and t_i the detection time of the i-th pulse. While the TES response to multiphoton events is not really linear, this model will give a reasonably good estimation of the timing for single photon absorption events.

— perfectly ?

A. Single photon pulse model

We obtain a model for the single photon response $v_1(t)$ of the TES and its signal amplification chain for the fit in Eq. 4 by selecting $N_1 = 10^4$ single photon traces from the measurement shown in figure 4, and averaging over them. The averaging process eliminates the noise from individual traces, and retains the detector response.

Signal photon events can happen at any time within the sampling window. It is necessary to align these detection events to average the traces. We assign a detection time to the i-th trace $v_1^{(i)}(t)$ by recording the time t_i corresponding to the maximum of $dv_1^{(i)}(t)/dt$. We use a Savitzky-Golay filter (SGF) to reduce the high frequency components[17]: the SGF replaces every point with the result of a fit of a line to the subset of adjacent 41 points.

We also reject clear outlier traces by limiting the search for t_i to the time interval CD. The remaining N_1 traces are then averaged by synchronizing them according the respective t_i to obtain the single-photon response $v_1(t)$,

$$v_1(t) = \frac{1}{N_1} \sum_{i=1}^{N_1} v_1^{(i)}(t + t_i). \qquad (5)$$

The result is shown in figure 5, together with a noise interval derived from the standard deviation of N_1 single photon traces. The model demonstrates an average rise time of 116 ns from 10 % to 90 % of its maximum height. The relaxation time ($1/e$) of 635 ns corresponds to detector thermalization[18].

B. Time-tagging via least-square fitting

For every qualified trace, we assign a number of photons N according to the calculated area, and fit it with Eq. (4). The fit has $2 \times N$ free parameters: detection times t_i and amplitudes A_i, with $i = 1 \ldots N$. We bound t_i to the range CD (figure 2(c)), and restrict the sum of A_i to be consistent with the thresholds obtained from the area distribution

$$\frac{a_{N-1,N}}{\int_{t_C}^{t_E} |v_1(\tau)| \, d\tau} \leq \sum_{i=1}^{N} A_i \leq \frac{a_{N,N+1}}{\int_{t_C}^{t_E} |v_1(\tau)| \, d\tau}. \qquad (6)$$

The accuracy of the fit depends on the choice of minimization algorithm. We used Powell's derivative-free method[19] because the presence of noise tends to corrupt gradient estimation[20].

To verify the accuracy of the fitting algorithm for $N = 2$, we expose the TES to pairs of short (4 ns) laser pulses with a controlled delay Δt_d that occasionally leads to traces with two overlapping detection pulses. The repetition rate of 100 kHz is low enough to isolate the TES
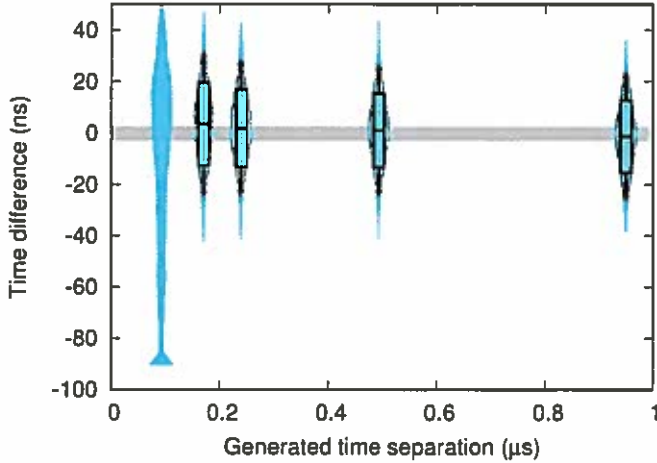
FIG. 7. Time difference between the expected and estimated detection-time separation of overlapping TES pulses generated by pairs of pulses from a LD. Blue region: Distribution of the time differences. Candlestick plots indicate mean and one standard deviation. Whiskersplots contain 90% of distribution. Grey region: The expected range of separation for 90 % of the two single-photon events that we generated using 4 ns wide LD pulse pairs. The TES pulses had rise-time of $\tau_{\mathrm{rise}} = 100$ ns in this experiment.
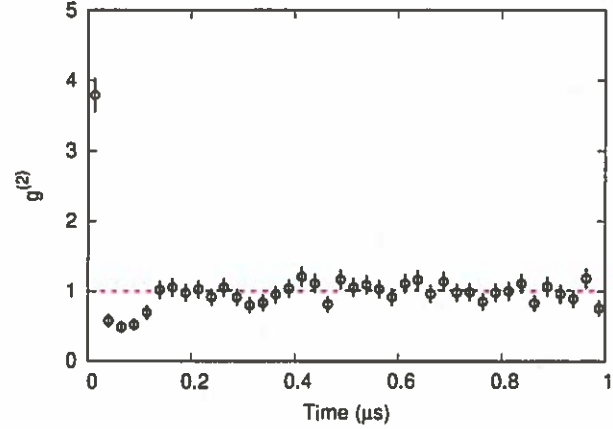

FIG. 8. Normalized detection-time separation histogram of a continuously running LD. Bin size = 25 ns. Error bars indicate Poissonian standard deviation. Red line: Theoretical prediction. The TES pulses had rise-time $\tau_{\mathrm{rise}} = 116$ ns in this experiment.

response between consecutive laser pulse pairs. While each pulse pair can generate two single photon events separated by Δt_d, they can also generate a single two-photon event in just one of the pulses (i.e., two detection events that can not be temporally resolved).

We compared the TES response for five different delays Δt_d: 92 ns, 170 ns, 239 ns, 493 ns, and 950 ns. Figure 6 shows an example of a measured trace where the fitting algorithm was able to distinguish between separate photodetection events at $\Delta t_d = 239$ ns even though it appears to be a single event because of the detector noise. For each delay we collected $\approx 3.5 \times 10^5$ traces, and for each trace we time tag the detection events using the least-square method. In figure 7 we summarize the distribution of time differences $\Delta t = |t_2 - t_1|$ for each delay.

Except for the shortest pulse separation, the time differences have Gaussian distributions with standard deviations of ≈ 16 ns. This is shows that extracting the timing information with the fit algorithm does not only work for overlapping pulses, but has also a higher accuracy than what the simple noise/slope estimation for the leading edge of the TES signal predicts.

The average separation between the center of the distribution and the expected result, $\Delta t - \Delta t_d$ is 2 ± 2 ns. For $\Delta t_d = 92$ ns, the distribution is clearly skewed toward 0 ns, indicating that the fit procedure is unable to distinguish two single-photon events generated by the two separated diode pulses from two-photon events generated within the same diode pulse.

VI. DETECTION-TIME SEPARATION FROM COHERENT SOURCE

As another benchmark for the fitting technique presented in here, we extract the normalized second order correlation function $g^{(2)}(\Delta t)$ for photodetection events recorded with a single TES from a coherent light field. For a light field in a coherent state, this correlation function should be exactly 1 for all time differences Δt[16].

For this, the TES is exposed to light from a continuously running laser diode, with an average photon number of about 0.3 per integration interval of around 3 μs. Again, we select only two-photon traces using the methods described in section IV, and fit the traces to the model described by equation 4 with $N = 2$.

Each fitted trace leads to two time values t_1 and t_2, which we sort into a frequency distribution $G^{(2)}(\Delta t)$ of time differences $\Delta t = t_2 - t_1$. We normalize this distribution with the distribution expected for a Poissonian source, taking into account the finite time of our acquisition windows. We further remove single-photon traces mis-identified as two-photon traces by filtering out traces that have a minimum estimated amplitude smaller than 0.5 times that of a single photon pulse.

The resulting normalized distribution $g^{(2)}(\Delta t)$ is shown in figure 8. For $\Delta t > 175$ ns, the correlation function is compatible with the expected value of 1. For shorter time differences, the fit algorithm occasionally locks the on the same detection times t_1 and t_2, redistributing pair events to $\Delta t = 0$. This instability region is comparable with twice the rise time of the average single-photon pulse in this acquisition, and is consistent with the precision indicated in figure 7.

VII. CONCLUSION

We demonstrated a signal processing method based on a Schmitt-trigger based data acquisition and a linear algorithm that can reliably extract both a photon number and photodetection times from the signal provided by an optical Transition Edge Sensor (TES) with an accuracy that is mostly limited by the detector time jitter.

Using this method, we successfully resolved between $n = 0, 1$ and 2 photons from a CW NIR source, using the signal integral evaluated in the time interval identified by the discriminator. The time interval includes a greater fraction of the photodetection signal than that considered by a single-threshold discriminator. By considering an optimal fraction of the pulse profile, we obtained pulse integral distributions that sufficiently resolve between photon numbers. This technique provides an alternative to photon counting using edge detection on the differentiated signal[10] when signal-to-noise ratio is low.

The discriminated region is then used to initialize a least-squares fit of a signal containing two overlapping TES pulses to a two-photon model, returning the amplitudes and detection-times of the individual photons.

With the available TES, we can distinguish two photodetection events within about 200 ns using this method. The highest detection rate that can be processed is thus estimated to be about 5×10^6 events/s, compared to about 4×10^5 events/s if we were to discard overlapping pulses.

Potential applications include the measurement of time-resolved correlation functions using the TES without the need for the spatial multiplexing of several single-photon non-photon-number resolving detectors, provided that the coherence time of the light source is larger than the timing resolution of this technique. The order of the correlation function measured is limited only by the maximum number of photons resolvable by the TES.

[1] A. E. Lita, B. Calkins, L. A. Pellouchoud, A. J. Miller, and S. Nam, SPIE Defense, Security, and Sensing **7681**, 76810D (2010).

[2] D. Fukuda, G. Fujii, T. Numata, K. Amemiya, A. Yoshizawa, H. Tsuchida, H. Fujino, H. Ishii, T. Itatani, S. Inoue, and T. Zama, Opt. Express **19**, 870 (2011).

[3] M. Giustina, M. A. M. Versteegh, S. Wengerowsky, J. Handsteiner, A. Hochrainer, K. Phelan, F. Steinlechner, J. Kofler, J.-A. Larsson, C. Abellán, W. Amaya, V. Pruneri, M. W. Mitchell, J. Beyer, T. Gerrits, A. E. Lita, L. K. Shalm, S. W. Nam, T. Scheidl, R. Ursin, B. Wittmann, and A. Zeilinger, Phys. Rev. Lett. **115**, 250401 (2015).

[4] Lamas-Linares, Antía, B. Calkins, N. A. Tomlin, T. Gerrits, A. E. Lita, J. Beyer, R. P. Mirin, and S. Nam, Appl. Phys. Lett. **102**, 231117 (2013).

[5] Z. H. Levine, T. Gerrits, A. L. Migdall, D. V. Samarov, B. Calkins, A. E. Lita, and S. W. Nam, J. Opt. Soc. Am. B **29**, 2066 (2012).

[6] S. Marrone, E. Berthomieux, F. Becvar, D. Cano-Ott, N. Colonna, C. Domingo-Pardo, F. Gunsing, R. C. Haight, M. Heil, F. Käppeler, M. Krtička, P. Mastinu, A. Mengoni, P. M. Milazzo, J. O'Donnell, R. Plag, P. Schillebeeckx, G. Tagliente, J. L. Tain, R. Terlizzi, and J. L. Ullmann, Nuclear Instruments and Methods in Physics Research, Section A: Accelerators, Spectrometers, Detectors and Associated Equipment **568**, 904 (2006).

[7] F. Belli, B. Esposito, D. Marocco, M. Riva, Y. Kaschuck, and G. Bonheure, Nuclear Instruments and Methods in Physics Research Section A: Accelerators, Spectrometers, Detectors and Associated Equipment **595**, 512 (2008).

[8] M. Vencelj, K. Bučar, R. Novak, and H. J. Wörtche, Nuclear Instruments and Methods in Physics Research, Section A: Accelerators, Spectrometers, Detectors and Associated Equipment **607**, 581 (2009).

[9] G. Tambave, E. Guliyev, M. Kavatsyuk, F. Schreuder, and H. Löhner, IEEE Nuclear Science Symposium Conference Record , 2163 (2012).

[10] J. W. Fowler, B. K. Alpert, W. B. Doriese, D. A. Fischer, C. Jaye, Y. I. Joe, G. C. O'Neil, D. S. Swetz, and J. N. Ullom, ApJS **219**, 35 (2015).

[11] A. E. Lita, A. J. Miller, and S. W. Nam, Opt. Express **16**, 3032 (2008).

[12] K. D. Irwin, Appl. Phys. Lett. **66**, 1998 (1995).

[13] D. Drung, C. Assmann, J. Beyer, A. Kirste, M. Peters, F. Ruede, and T. Schurig, IEEE Trans. Appl. Supercond. **17**, 699 (2007).

[14] O. H. Schmitt, J. Sci. Instrum. **15**, 24 (1938).

[15] B. Cabrera, R. Clarke, A. Miller, S. W. Nam, R. Romani, T. Saab, and B. Young, Physica B: Condensed Matter **280**, 509 (2000).

[16] R. J. Glauber, Phys. Rev. **130**, 2529 (1963).

[17] A. Savitzky and M. Golay, *Analytical chemistry*, **36**, 1627 (1964).

[18] A. E. Lita, B. Calkins, L. A. Pellouchoud, A. J. Miller, and S. W. Nam, SPIE Defense, Security, and Sensing **7681**, 76810D (2010).

[19] M. J. D. Powell, The Computer Journal **7**, 155 (1964).

[20] V. P. Plagianakos and M. Vrahatis, *Combinatorial and Global Optimization* (2002) pp. 283–296.